IL NUOVO CIMENTO Vol. 30 C, N. 4 Luglio-Agosto 2007
DOI 10.1393/ncc/i2007-10251-9

# Evaluation of the dispersion coefficient for numerical simulations of tropospheric transport

F. Tampieri(*) and A. Maurizi
*ISAC-CNR - Bologna, Italy*

(ricevuto il 18 Novembre 2007; approvato il 2 Dicembre 2007; pubblicato online il 2 Febbraio 2008)

**Summary.** — Data of velocity spectra in wave number and frequency space available in literature are analysed to estimate climatological values of the dissipation rate of kinetic energy $\varepsilon$. In the frame of Kolmogorov (1941) theory, the relationship between diffusion coefficient and spectral window is used to determine the diffusion coefficient as a function of resolved scale. To exploit frequency spectrum data with a limited knowledge of flow conditions, a hypothesis on the relationship between the Eulerian time scale and the sampling temporal window was formulated, and the implied empirical constant was determined. Using the obtained values and some recent similarity relationships for the boundary-layer, a parameterisation of $\varepsilon$ was adopted to propose an expression of the horizontal dispersion coefficient for different heights and different scales, which is suitable for use in numerical models with special reference to climate applications.

PACS 47.27.T- – Turbulent transport processes.
PACS 47.27.tb – Turbulent diffusion.
PACS 92.60.Aa – Modeling and model calibration.
PACS 92.10.Lq – Turbulence, diffusion, and mixing processes in oceanography.
PACS 92.60.hk – Convection, turbulence, and diffusion.

## 1. – Introduction

Transport processes in geophysical flows are of great interest for many applications, from climate change to air quality issues. The numerical simulation of tracer dispersion in the atmosphere is a task of increasing significance in the numerical modelling of the chemical composition of the atmosphere.

Tracer dispersion in the free troposphere is affected mainly by the horizontal velocity field, while vertical transport becomes relevant only in the presence of deep convection phenomena.

(*) E-mail: f.tampieri@isac.cnr.it

 

In numerical models, horizontal dispersion can be described in terms of a diffusion coefficient $D_h$ related to the unresolved (subgrid) part of the velocity field. This coefficient can be used directly in the advection-diffusion equation, or to obtain the amplitude of the random noise in a trajectory approach.

The concept of a diffusion coefficient related to unresolved motion implies that the spatial and temporal discretisation is finer than the corresponding scales of variation of the transported quantity (see *e.g.*, [1]). This limits the application to resolutions that are much finer than the source extension. Nevertheless, the concept is widely used even beyond this limit.

In general, dissipation, variance and mean field are functions of space and time, as is the diffusion coefficient. However, estimates of this coefficient from "climatological" observations , *i.e.* obtained in a variety of scales and different flow conditions, can highlight some general features and offer simple parameterisations for practical applications.

$D_h$ can be estimated at a given resolution when the properties of turbulence at the scale of the resolution are known. It can be determined from velocity spectra measured in a variety of flow conditions and experimental arrangements.

Although there are still open questions on the existence and nature of a $k^{-3}$ slope for very large scales, as well as on the nature of the $k^{-5/3}$ slope in the mesoscale range [2-4], a range of $k^{-5/3}$ is common in observations. Literature spectra concerning the troposphere will be examined in a Kolmogorov (1941) [5] perspective.

The inertial subrange part of the spectrum will be used to estimate $\varepsilon$ and, thus, the velocity variance for wave numbers larger than a given $k$ (or frequencies larger than a given $f$). A time scale can be derived from $k$ spectra or argued from frequency data. Subsequently, the diffusion coefficient appropriate for the scale $k$ (or $f$) is computed.

## 2. – Evaluation of the eddy dispersion coefficient from wave number spectra

Assuming the existence of an inertial subrange characterised by the spectrum

$$E(k) = C_1 \varepsilon^{2/3} k^{-5/3}, \tag{1}$$

where $C_1 \simeq 0.25 C_K$, $\varepsilon$ may be derived by fitting

$$\varepsilon = E(k)^{3/2} C_1^{-3/2} k^{+5/2} \tag{2}$$

to $E(k)$ observations. The variance of the velocity is given by

$$\sigma^2(k) = \int_k^{k_\eta} E(k)\mathrm{d}k = C_1 \varepsilon^{2/3} \int_k^{k_K} k^{-5/3}\mathrm{d}k \tag{3}$$

and, provided the viscous wave number $k_\eta$ is large enough, which is the case in geophysical flows:

$$\sigma^2(k) \simeq \frac{3}{2} C_1 \varepsilon^{2/3} k^{-2/3}\,. \tag{4}$$

A time scale can be determined using the Lagrangian structure function for the inertial subrange, assuming an exponential form of the correlation function:

$$\tau_L(k) \equiv \frac{2\sigma^2(k)}{C_0 \varepsilon} = \frac{3C_1}{C_0} \varepsilon^{-1/3} k^{-2/3}\,. \tag{5}$$

An estimate of the eddy dispersion coefficient as a function of the wave number is given by

$$D_h(k) = \tau_L(k)\sigma^2(k) \tag{6}$$

which using eq. (5) reads

$$D_h(k) = \frac{9}{2}\frac{C_1^2}{C_0}\varepsilon^{1/3}k^{-4/3}\,. \tag{7}$$

## 3. – Evaluation of eddy dispersion coefficient from frequency spectra

Measurements are more frequently available as time series taken at a fixed point. Time series are usually analysed as Eulerian measurements in space, invoking the Taylor frozen turbulence hypothesis.

From the spectrum written as a function of frequency $f$

$$E(f) = Kf^{-5/3}, \tag{8}$$

where

$$K = C_2\overline{u}^{2/3}\varepsilon^{2/3} \tag{9}$$

with $C_2 = C_1/(2\pi)^{2/3}$, an expression for $\sigma^2(f)$ in the inertial subrange can be obtained:

$$\sigma^2(f) \simeq \frac{3}{2}C_2\overline{u}^{2/3}\varepsilon^{2/3}f^{-2/3} = \frac{3}{2}Kf^{-2/3}\,. \tag{10}$$

The time scale reads, assuming $\varepsilon$ constant,

$$\tau_L(f) \equiv \frac{2\sigma^2(f)}{C_0\varepsilon} = \frac{3C_2\overline{u}^{2/3}}{C_0}\varepsilon^{-1/3}f^{-2/3}\,. \tag{11}$$

The value of $K$ can be obtained by fitting eq. (8) to data, but an estimate of the mean velocity specific for each case is necessary, which is not always available from published data.

From fixed point time series measurements the value of the Eulerian time scale $\tau_E$ can be derived. In general, $\tau_E$ is a function of the sampling length, *i.e.* of the lowest resolved frequency $\tilde{f}$ (see, *e.g.*, [6]). It is assumed here that the relationship between $\tau_E$ and $\tau_L$ is independent of $\tilde{f}$. Therefore, $\tau_E$ can be derived from $\beta = \tau_L/\tau_E$, the Lagrangian-to-Eulerian scale ratio [7], once the value of $\beta$ is known.

It can be observed that if $\beta$ is defined in terms of inertial subrange properties [8] as

$$\beta = \frac{C_K^{3/2}}{\sqrt{2}C_0} \tag{12}$$

which is independent of any large scale feature and therefore of $\tilde{f}$. Thus, through eq. (12) the following is obtained:

$$\tau_E(f) = \frac{3\sqrt{2}C_2}{C_K^{3/2}}\varepsilon^{-1/3}\overline{u}^{2/3}f^{-2/3}, \tag{13}$$

where the explicit dependence on the mean velocity appears.

Lacking in general the possibility of a direct computation of $\tau_E$ from published data, some hints can be derived from the papers by Maryon [6] and Anfossi *et al.* [9], which focus on meandering.

Maryon [6] examines 10 minute averages of time series of wind measured at 21 m in Cardington (UK) over a long period. Statistics over 12 h, 6 h and 2 h are then computed by moving average for each period of 1 month.

The variances of the transversal component referring to the different averaging periods are obtained by integrating the spectrum from the maximum frequency to the frequency corresponding to the chosen period. The time correlations are determined from the integral of the correlation from 0 to the time at which the correlation first reduces to zero.

Again with reference to meandering, table I from [9] gives some additional values for the relation between sampling time and meandering period $T_*$ (assumed here to be a measure of the time scale).

According to eq. (13), the correlation time is related to the averaging window frequency. The relationship

$$\tau_E = \alpha f^{-2/3} \tag{14}$$

can be tested against the data (identifying $\tilde{f} = \Delta T^{-1}$ or $\tilde{f} = 2\Delta T^{-1}$, and $\tau_E = T_*$ or $\tau_E = \tau_m$ for [9], or [6], respectively), although it is not possible here to assess the dependences of

$$\alpha = \frac{3\sqrt{2}C_2}{C_K^{3/2}} \varepsilon^{-1/3} \overline{u}^{2/3} \tag{15}$$

from the flow characteristics. However, the data reported in fig. 1 support the validity of a constant $\alpha$, and fitting eq. (14) to data gives $\alpha \simeq 3.8$ (see fig. 1). What can be assumed is that the value obtained is somewhat representative of the climatology for the low frequency (mesoscale) part of the spectrum.

Assuming a constant value of $\alpha$ for a given spectral range (characterised by a unique $k^{-5/3}$ slope) is equivalent to assuming that $\overline{u}^2$ is a measure of the energy introduced in the system (via shear instabilities), and $\varepsilon$ is the local dissipation of that energy. Experimental observations show that in geophysical flows at least two different $k^{-5/3}$ ranges appear. Different spectral ranges may have different values of $\alpha$.

Using eq. (15), the mean velocity in eq. (9) can be eliminated, obtaining an expression for $\varepsilon$:

$$\varepsilon = \frac{3\sqrt{2}K}{\alpha C_2 C_K^{3/2}} , \tag{16}$$

where $K$ is specific for each flow.

The dispersion coefficient as a function of frequency can be obtained using eq. (7) written in terms of $f$, and using eq. (10):

$$D_h(f) = \frac{9K^2}{2C_0\varepsilon} f^{-4/3} = \frac{9}{2} \frac{C_2^2}{C_0} \overline{u}^{4/3} \varepsilon^{1/3} f^{-4/3} . \tag{17}$$

This expression is the same as eq. (7) with the transformation $k = 2\pi f/\overline{u}$.

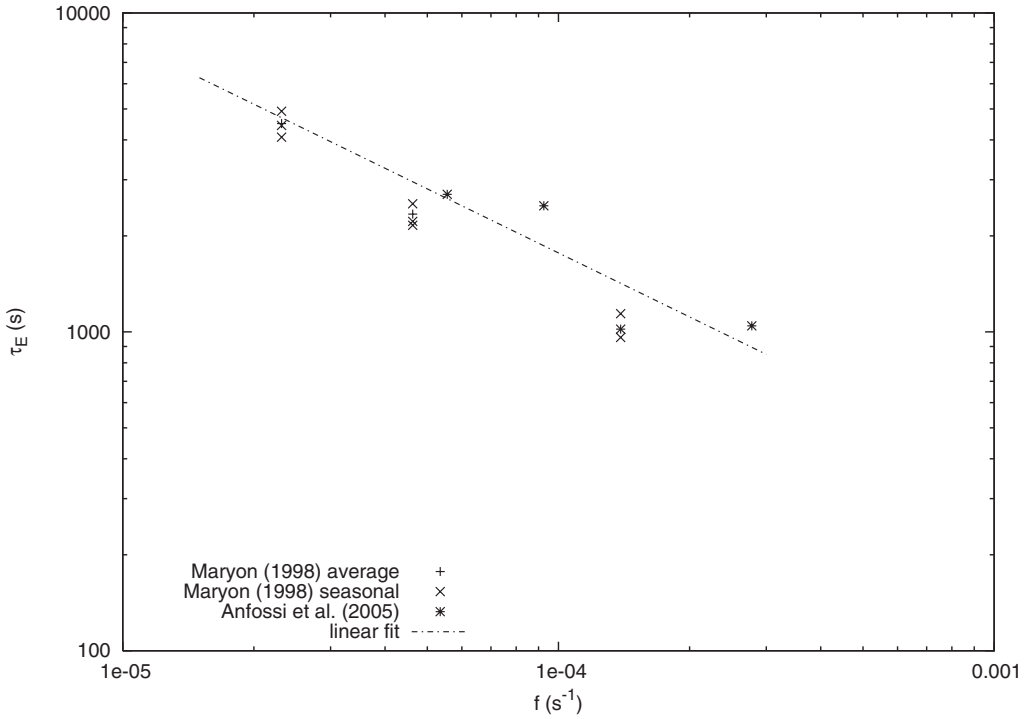


Fig. 1. – $\tau_E(f)$ as function of $f$, from the data of [9] and [6].

## 4. – $\varepsilon$ estimates

A number of spectra from literature were analysed. The following wave number spectra from literature were considered.

Gage [2] summarises earlier works on the mesoscale spectrum of the atmosphere. With special reference to Lilly and Petersen [10], he presents an envelope of spectra referring to the upper half of the troposphere, showing a $k^{-5/3}$ slope in the range $10^{-5}\,\mathrm{m}^{-1} < k < 10^{-3}\,\mathrm{m}^{-1}$.

Cho *et al.* [11] presents aircraft measurements averaged according to two height intervals ($z < 1000\,\mathrm{m}$, $1000\,\mathrm{m} < z < 5000\,\mathrm{m}$), and over a wide latitudinal range. The $k^{-5/3}$ slope was identified in the ranges $0.1\,\mathrm{km}^{-1} < k/(2\pi) < 3\,\mathrm{km}^{-1}$ and $0.05\,\mathrm{km}^{-1} < k/(2\pi) < 3\,\mathrm{km}^{-1}$ for the two height intervals, respectively.

Högstrom *et al.* [12] (their fig. 10) present wave number spectra averaged between 30 and 350 m (measured during strong stability conditions), which show a $k^{-5/3}$ slope in the range $2 \times 10^{-4}\,\mathrm{m}^{-1} < k < 2 \times 10^{-3}\,\mathrm{m}^{-1}$. The authors observe that the amplitude of the spectrum is about a factor of 2 less than in [2]. Accordingly, the dissipation rate turns out to be smaller (see fig. 2).

Among the many frequency spectra presented in the literature, only a limited number cover the range of low frequencies. A sample of available data is presented below.

Van der Hoven [13] is a classical reference: a composite spectrum of wind in the surface layer (10 m). The data have been fitted with the $f^{-5/3}$ line in two ranges: low frequencies $0.01\,\mathrm{h}^{-1} < f < 0.05\,\mathrm{h}^{-1}$; high frequencies $50\,\mathrm{h}^{-1} < f < 1000\,\mathrm{h}^{-1}$.

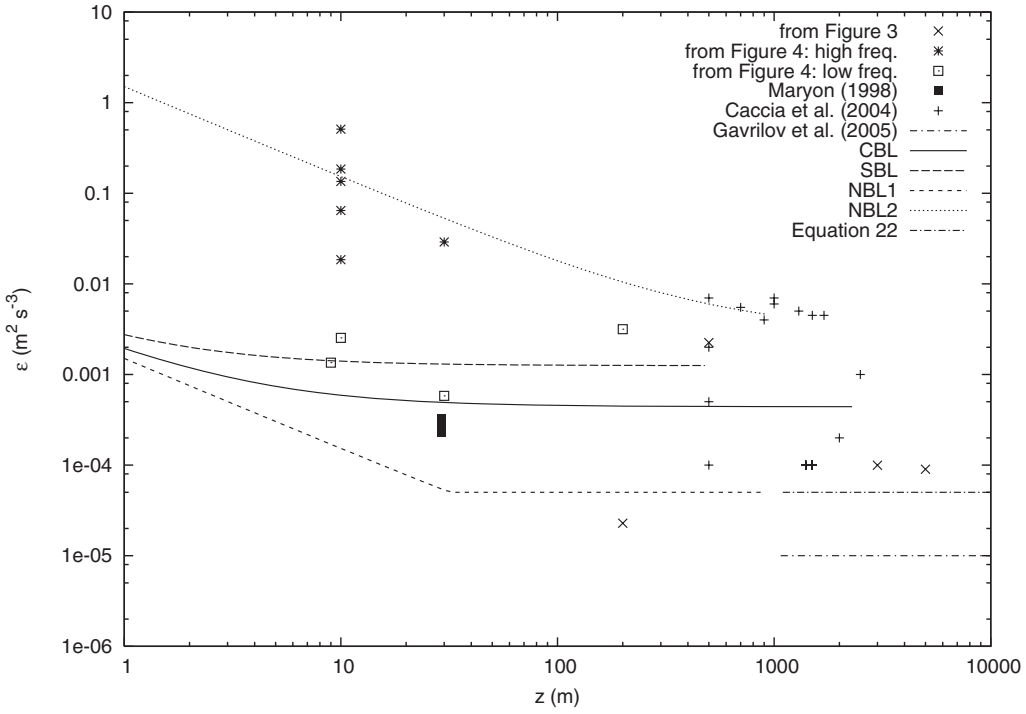


Fig. 2. – Estimates of $\varepsilon$ (in $\mathrm{m^2 s^{-3}}$).

Courtney and Troen [14] report a spectrum from one year of data taken at 30 m above the ground. Again, two frequency ranges are considered: $5 \times 10^{-2}\,\mathrm{s^{-1}} < f < 1\,\mathrm{s^{-1}}$ and $10^{-6}\,\mathrm{s^{-1}} < f < 5 \times 10^{-4}\,\mathrm{s^{-1}}$.

Masmoudi and Weill [15] present spectra in the boundary layer derived from SODAR measurements. A spectrum averaged over a layer 350 m thick and four stations (their fig. 3d), in the frequency range $10^{-5}\,\mathrm{s^{-1}} < f < 10^{-4}\,\mathrm{s^{-1}}$, is used here.

Högstrom *et al.* [12] present an envelope of frequency spectra taken at 9 m above the ground, in the range $5 \times 10^{-5}\,\mathrm{s^{-1}} < f < 10^{-3}\,\mathrm{s^{-1}}$ (their fig. 11).

A few surface layer spectra are also reported by Anfossi *et al.* [16], their fig. 5, and Anfossi *et al.* [9], their fig. 5. All these data (spectra averaged over many realizations) refer to surface layer measurements (6.8 m high in the first case, 10 m, cross-wind component in the second) with frequencies ranging from $4 \times 10^{-1}\,\mathrm{s^{-1}} < f < 3\,\mathrm{s^{-1}}$ and $9 \times 10^{-2}\,\mathrm{s^{-1}} < f < 4 \times 10^{-1}\,\mathrm{s^{-1}}$, respectively.

Estimations of $\varepsilon$ in the troposphere were carried out using data from both wave number and frequency spectra. Spectra in wave number space provide a straightforward way to compute $\varepsilon$ through eq. (2), for $C_K = 2$. By contrast, in order to evaluate $\varepsilon$ from spectra in frequency space, eq. (16) is used in conjunction with the assumption of a constant $\alpha$ based on data reported in fig. 1.

From eq. (11):

$$\varepsilon = \frac{2\sigma^2(f)}{C_0 \beta \tau_E(f)} = \frac{\sigma^2(f)}{\tau_E(f)}\,. \tag{18}$$

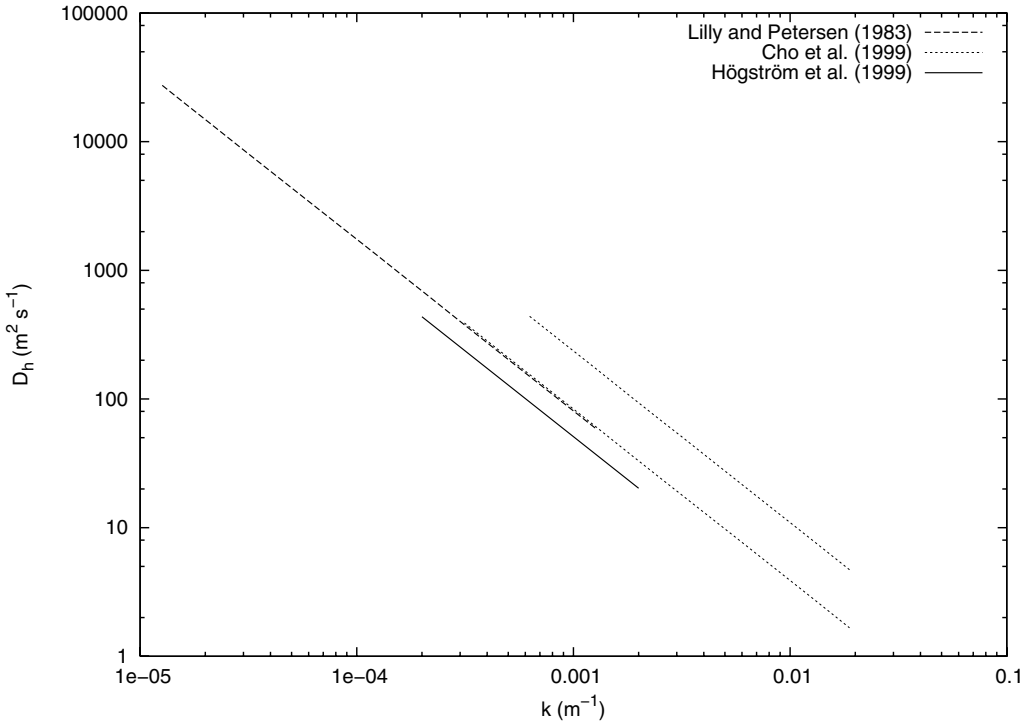


Fig. 3. – Eddy dispersion coefficient as a function of wave number obtained from different authors (see text).

Using the values of variance and time scale from Marion's table 5, an overall value for the dissipation is obtained: $\varepsilon \simeq 2.9 \times 10^{-4}\,\mathrm{m^2 s^{-3}}$. Note that a dependence on seasonal conditions could be investigated using the data from tables 2, 3 and 4. It turns out that the winter values (around $3.2 \times 10^{-4}\,\mathrm{m^2 s^{-3}}$) are systematically slightly higher than the summer ones (around $2.7 \times 10^{-4}\,\mathrm{m^2 s^{-3}}$; see fig. 2). A summary of the estimates of $\varepsilon$ is reported in fig. 2. Note that the median value obtained by [10] is $9 \times 10^{-5}\,\mathrm{m s^{-1}}$, while the one reported by [17] for the troposphere is $10^{-5}\,\mathrm{m s^{-1}}$. A set of values estimated by [18] is also reported (including cases of convection, characterised by higher dissipation values with respect to the typical value at the same height).

Estimates of the horizontal diffusion coefficient are reported in figs. 3 and 4 for wave number and frequency spectra, respectively. Note that in eq. (7) and eq. (17), $C_0 = 6.2$ was assumed [19].

It can be observed that the energy density associated to boundary-layer turbulence is higher than that observed in the free troposphere. This corresponds to a higher diffusivity for measurements taken at lower heights, as can be seen in fig. 3 looking at the [11] data measured at different levels. The existence of two regimes is also observed in frequency space (fig. 4), and is consistent with oceanic observations [20, p. 215].

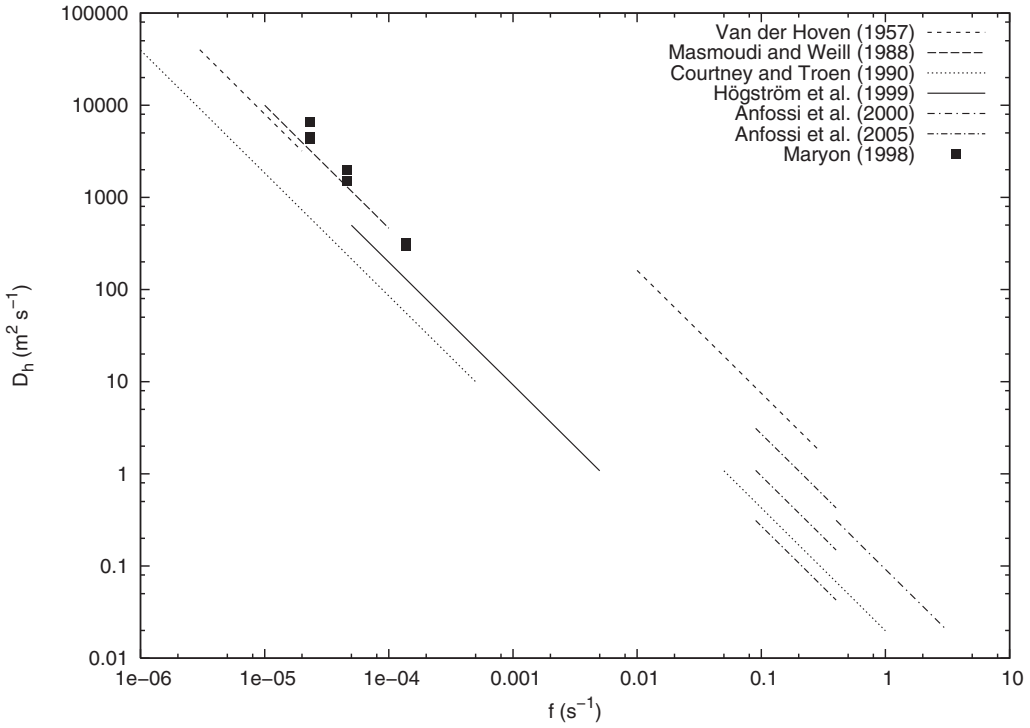


Fig. 4. – Eddy dispersion coefficient as a function of frequency obtained from different authors (see text).

## 5. – A parameterisation for $D_h$

In order to apply the previous results to numerical models, a simple parameterisation for the diffusion coefficient, as a function of the horizontal resolution and of the height, can be suggested. To compute it, use is made of the similarity expressions for the dissipation rate $\varepsilon$ in the boundary layer, and a fixed value derived from data in the free troposphere.

TABLE I. – *Parameters used for different stabilities in the boundary layer.*

| | $u_*$ ($ms^{-1}$) | $L_{MO}$ (m) | $h_{bl}$ (m) |
|---|---|---|---|
| CBL | 0.1 | $-10$ | 2500 |
| SBL | 0.1 | $+10$ | 500 |
| NBL1 | 0.1 | $\infty$ | 1000 |
| NBL2 | 1.0 | $\infty$ | 1000 |

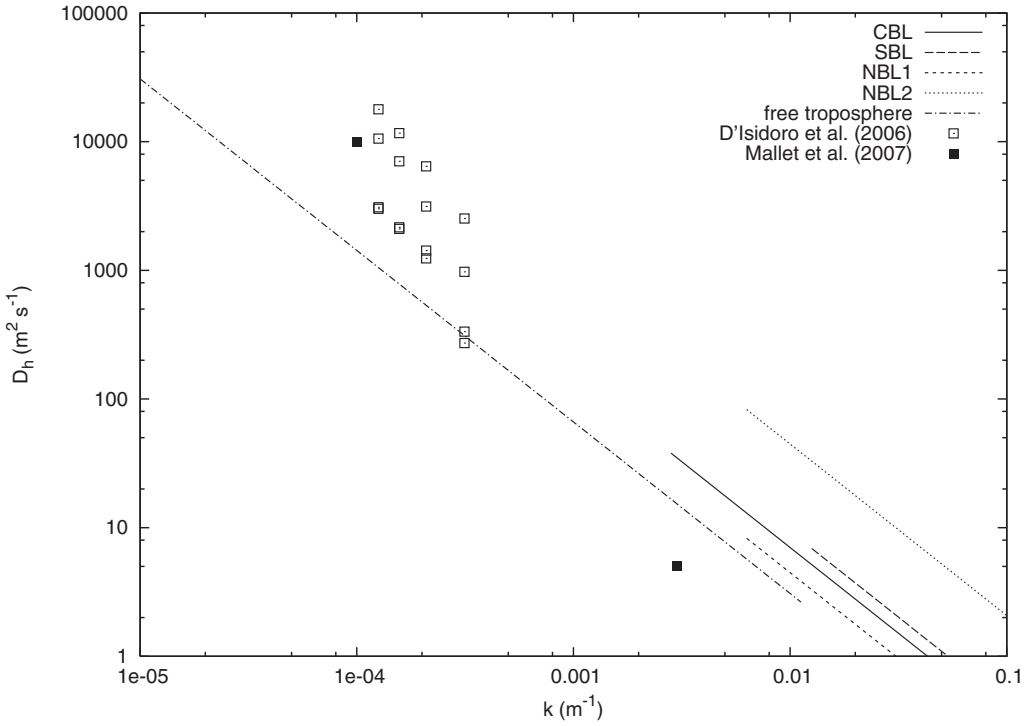


Fig. 5. – Diffusion coefficient as a function of wave number for the proposed parameterisation of $\varepsilon$ (eqs. (19) and (20)) computed for $z = 10\,\mathrm{m}$.

Unstable conditions yield

$$\varepsilon = \frac{u_*^3}{\kappa \tilde{z}} \left( 0.61 - 1.75 \frac{\tilde{z}}{L_{MO}} \right), \; L_{MO} < 0 \tag{19}$$

[21], and stable conditions give

$$\varepsilon = \frac{u_*^3}{\kappa \tilde{z}} \left( 0.61 + 5 \frac{\tilde{z}}{L_{MO}} \right), \; L_{MO} > 0 \tag{20}$$

[22] where

$$\tilde{z}^{-1} = \ell_0^{-1} + z^{-1} \tag{21}$$

in which $\ell_0 = 500\,\mathrm{m}$ is assumed.

The previous expressions hold within the boundary layer ($z < h$). Above this layer

$$\varepsilon = 5.10^{-5}\,\mathrm{m^2 s^{-3}} \tag{22}$$

is assumed as being representative of tropospheric data, and is also assumed as the minimum. For model applications, the height $h$ can be determined case by case, using

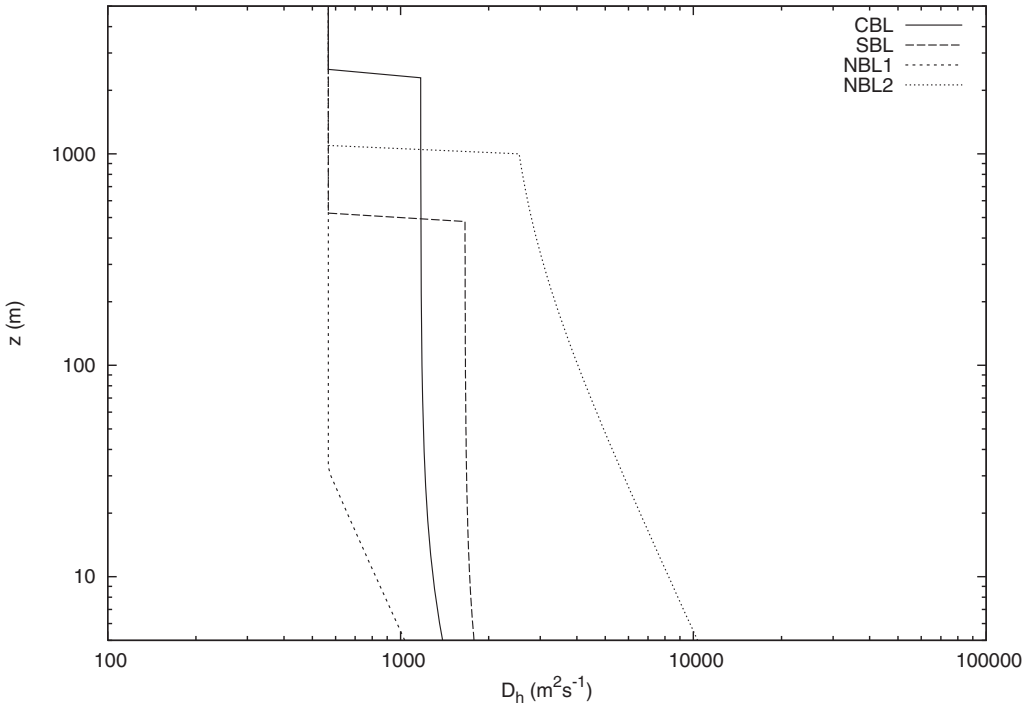


Fig. 6. – Diffusion coefficient as a function of height for the proposed parameterisation of $\varepsilon$ (eqs. (19) and (20)) computed for $k = 2 \times 10^{-4}\,\mathrm{m}^{-1}$.

model profiles along with the actual stability. Some sample curves for stable, convective and neutral cases are reported in fig. 2, while the values assumed for parameters in different cases are reported in table I.

To estimate the horizontal diffusion coefficient, eq. (7) is used, substituting the proper expression for the dissipation rate. Different dissipation rates are appropriate for small and large wave number ranges. The separating values between small and large wave numbers are identified with the expression $k_h = 2\pi/h$. The height $z$ for the computation of $\varepsilon$ should be the measurement height for boundary layer observations concerning the large wave number range; in the small wave number range the typical tropospheric value for $\varepsilon$ is recommended, regardless of the value of $z$.

Some sample results, for the same combinations between stability and friction velocity as in fig. 2, are reported in figs. 5 and 6. This parameterisation evidences clear the discontinuity of $D_h$ at scales corresponding to the boundary layer height.

For comparison with numerical simulations, values of $D_h$ taken from [23] are reported in fig. 5. As a further reference, [24] have shown that, using a transport equation, with or without hyper-diffusion $\nabla^4$, gives rise to a diffusion-like process. Effective diffusivities from [24] are also reported in fig. 5.

## 6. – Conclusions

The analysis of spectral data from literature leads to the determination of $\varepsilon$ for different heights. Using the obtained values and some recent similarity relationships for

the boundary-layer, a parameterisation of $\varepsilon$ has been proposed and used to derive an expression of the horizontal dispersion coefficient for different heights and different scales which is suitable for use in numerical models.

To determine $D_h$ from frequency spectra when mean velocity is not available, a hypothesis on a relationship between the Eulerian time scale and the sampling temporal window has been formulated. An empirical constant has been determined, which can be considered valid in a climatological sense, but whose validity should be verified with a more extensive dataset.

* * *

The authors acknowledge partial support from EC IP GEMS, the Italia-USA agreement for research on climate changes and the National Programme for Antarctic Research.

REFERENCES

[1] Corrsin S., *Adv. Geophys. A*, **18** (1974) 25.
[2] Gage K., *Dynamic processes contributing to the mesoscale spectrum of atmospheric motions*, *Atmospheric Turbulence and Mesoscale Meteorology*, edited by Fedorovich E., Rotunno R. and Stevens B. (Cambridge University Press) 2004.
[3] Gkioulekas E. and Tung K. K., *Discrete Contin. Dyn. Syst. - Ser. B*, **5** (2005) 103.
[4] Liechtenstein L., Godeferd F. S. and Cambon C., *Flow, Turbul. Combust.*, **76** (2006) 419.
[5] Kolmogorov A., *Dokl. Akad. Nauk SSSR*, **30** (1941) 301.
[6] Maryon R., *Atmos. Environ.*, **32** (1998) 115.
[7] Hinze J., *Turbulence* (Mc Graw-Hill, New York) 1959.
[8] Maurizi A., Pagnini G. and Tampieri F., *Boundary-Layer Meteorol.*, **118** (2006) 55.
[9] Anfossi D., Oettl D., Degrazia G., Ferrero E. and Goulart A., *Boundary-Layer Meteorol.*, **114** (2005) 179.
[10] Lilly D. and Petersen E., *Tellus A*, **35** (1983) 379.
[11] Cho J., Zhu Y., Newell R., Anderson B., Barrick J., Gregory G., Sachse G., Carroll M. and Albercook G., *J. Geophys. Res. D*, **104** (1999) 5697.
[12] Högström U., Smedman A.-S. and Bergstrom H., *J. Atmos. Sci.*, **56** (1999) 959.
[13] Van der Hoven J., *J. Meteorol.*, **14** (1957) 160.
[14] Courtney M. and Troen I., *Wind speed spectrum from one year of continuous 8 hz measurements*, in *Proc. 9th Symposium on Turbulence and Diffusion* (American Meteorological Society, Boston, Mass.) 1990.
[15] Masmoudi M. and Weill A., *J. Appl. Meteorol.*, **27** (1988) 864.
[16] Anfossi D., Degrazia G., Ferrero E., Gryning S., Morselli M. and Trini Castelli S., *Boundary-Layer Meteorol.*, **95** (2000) 249.
[17] Gavrilov N., Luce H., Crochet M., Dalaudier F. and Fukao S., *Ann. Geophys.*, **23** (2005) 2401.
[18] Caccia J., Guenard V., Benech B., Campistron B. and Drobinski P., *Ann. Geophys.*, **22** (2004) 3927.
[19] Ouellette N., Xu H., Bourgoin M. and Bodenschatz E., *New J. Phys.*, **8** (2006).
[20] Monin A. and Ozmidov R., *Turbulence in the Ocean* (D. Reidel Publ. Co., Dordrecht) 1985.
[21] Albertson J. D., Parlange M., Kiely G. and Eichinger W. E., *J. Geophys. Res.*, **102** (1997) 13423.
[22] Pahlow M., Parlange M. and Porte-Agel F., *Boundary Layer Meteorol.*, **99** (2000) 225.
[23] Mallet V., Pourchet A., Quelo D. and Sportisse B., *J. Geophys. Res.*, **112** (2007) 1.
[24] D'Isidoro M., Maurizi A., Tampieri F., Tiesi A. and Villani M., *Nuovo Cimento C*, **28** (2005) 151, on-line version `http://dx.doi.org/10.1393/ncc/i2005-10188-y`.